

Analysis of flow separation in the Western Scheldt estuary: remote sensing.

Léon Wijker, Earth Surface and Water, 6050387, 14/09/2024

supervisors: prof. dr. Maarten G. Kleinhans and dr. Maarten van der Vegt

Abstract

The Western Scheldt estuary, located in the south-east of the Netherlands, is an important shipping lane to and from the Port of Antwerp. Flow patterns are very complex, and zones with flow separation pose dangers to ships. There are currently no models that can predict flow separation for a longer period of time at such a large scale as the Western Scheldt estuary. Due to the importance of the estuary as a shipping lane, understanding the factors that lead to flow separation is eminent, but it is still not clear under which conditions flow separation develops. The aim of this thesis is therefore to empirically determine the hydro-morphological factors determining the point where flow separates in sharp corners of the Western Scheldt estuary, and properties of the flow separation zone in relation to the tidal phase and the morphology of the bed and bars. To that end, I applied remote sensing to satellite imagery of the Western Scheldt to study occurrence and properties of flow separation, focussing on the largest bend where this occurs frequently. Although literature suggests that the Froude number and the radius to width ratio is important for flow separation, they do not appear to be very useful for understanding flow separation in the Western Scheldt. Rather, hydro-morphological feedback mechanisms appear to be the dominant processes in the development of flow separation. The shape and location of the bars and the bathymetry are leading in the occurrence of separation zones, while larger water levels and accordingly higher flow velocities widen and strengthen the flow separation zones. Recirculation was found to occur in the flood phase in the lee of a sharp bend, particularly in shallow zones, where the ebb-return currents then develop faster than in the adjacent deeper channel. The ebb current erodes the east face of the Ossensisse shoal after which its flow separates around the apex in ebb direction, leading to recirculation at the west face of the shoal. This maintains the triangular shape of the shoal, which in turn provides the perfect circumstances for flow separation around the “sharp bend” at the apex of the Ossensisse shoal, completing the positive hydro-morphological feedback loop. These insights suggest that changing the morphology by depositing dredged material in the separating zone may reduce the flow separation, which may be useful for navigational safety and may be feasible in view of the large dredging volumes in the Western Scheldt.

Table of Contents

Abstract	1
1. Introduction	3
1.1 Flow separation.....	3
1.2 Effects of morphology on flow separation	6
1.3 Research questions.....	8
2. Methods	10
2.1 Used imagery	10
2.2 used data.....	11
3. Results.....	14
3.1 Trends and observations.....	14
3.2 Influence of changes in water depth.....	18
4. Discussion	21
4.1 Ebb dominated channel.....	21
4.2 Bend curvature.....	23
4.3 Turbulence.....	24
4.4 Morphology	26
Conclusions.....	28
Acknowledgements	28
References.....	29

1. Introduction

1.1 Flow separation

Flow separation occurs in rivers and estuaries of all scales around the world. Separation of the flow is not restricted to water however, as this process is also relevant in aerodynamics, where the separation of airflow behind the rear wing of a Formula 1 car causes eddies and drag. In the Western Scheldt estuary, flow patterns are very complex and hard to navigate without a thorough understanding of both flow and bed dynamics. The estuary is a very busy shipping lane, connecting the Channel to the port of Antwerp, with 66,701 ship movements in 2022 alone (Hermans et al., 2022). Because this is such a frequently used shipping lane, an increased understanding of flow dynamics in the estuary is vital for safety, maintenance and habitat quality and extent.

Although the process of flow separation has been known for a long time, there are currently no models that are able to predict flow separation for a longer period of time at a such a large scale as the Western Scheldt estuary. This is due to the fact that flow models require complex turbulence closure for the flow separation and possible recirculation to emerge (Kleinhans et al., 2023). There is in particular a lack of insight into the interactions between near-bank flow processes and their sedimentological and morphological effects (Blanckaert, 2018).

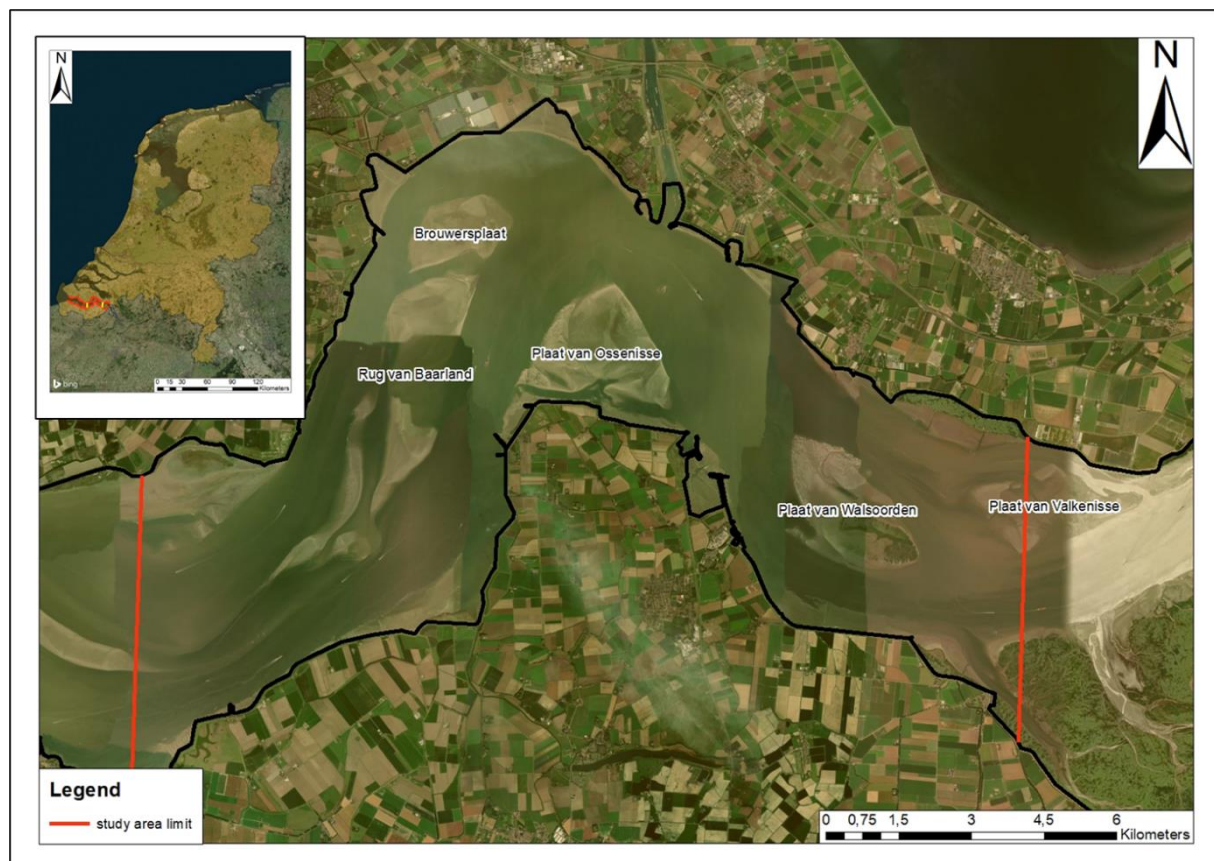


Figure 1: Study area, with from left to right: Baarland ridge, Brouwers shoal, Ossensisse shoal, Walsoorden shoal, Valkenisse shoal.

The area of interest is the Western Scheldt estuary (Dutch: Westerschelde) located in the south of the Netherlands (Figure 1). The estuary has a length of 65 kilometres and a channel depth of 13.4 to 51.4 metres under mean sea level, and several intertidal and supratidal bars and shore-connected tidal flats and saltmarshes (Rijkswaterstaat, 2024). The borders of the Western

Scheldt estuary are fixated by dikes and other bank protection works. The estuary is macrotidal with a semi-diurnal tidal regime. In the corner near Hansweert around the Ossenissee shoal (Figure 1), complex morphology and flow separation is present (Plancke et al., 2020) which leads to navigational difficulties.

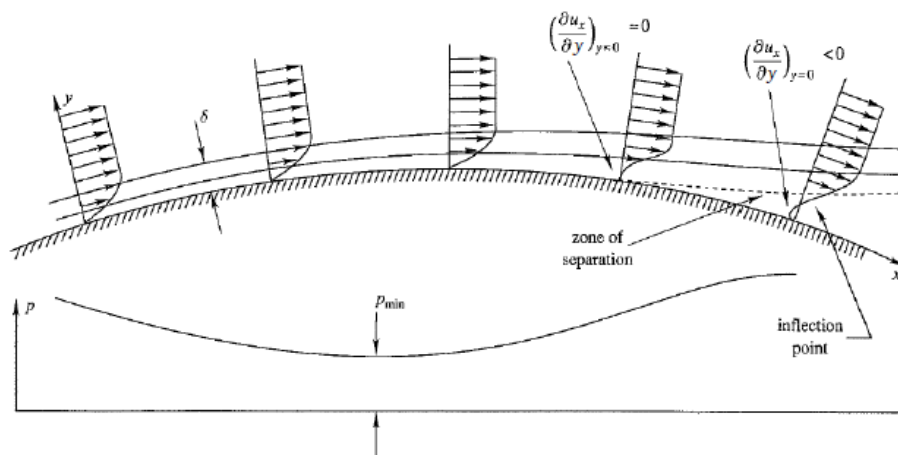
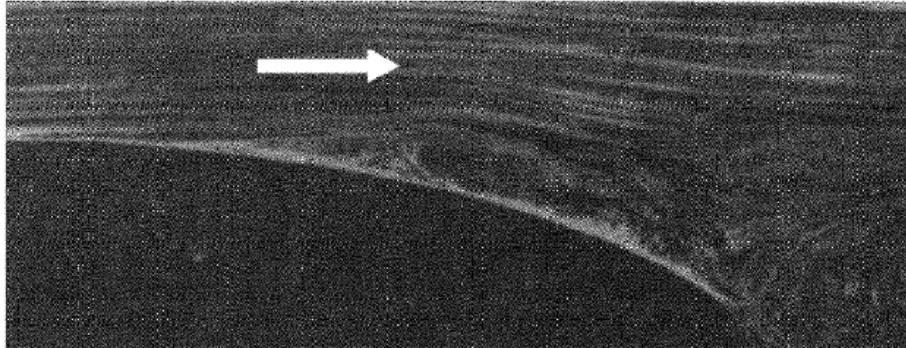


Figure 2: The boundary layer above a convex object (photo from Prandtl, 1952)

Similar to the definitions of Bagnold (1960); Leeder and Bridges 1975; Simpson (1989) and Blanckaert (2015), flow separation and recirculation are here defined as the separation of the flow of water from the inner bank, where a faster moving body of water is separated from a slower moving or even recirculating body of water by a shear layer (Figure 2). In line with Simpson (1989), separation is described as the entire process of *departure* or *breakaway*, or the breakdown of boundary-layer flow. When the water between the inner bank and the shear layer is still flowing in downstream direction, this is considered to be the first stage of flow separation (Figure 3c), whereby the streamwise flow velocity is no longer monotonously increasing away from the bank, but shows an inflection point (Figure 3a). The second stage of flow separation is reached when upstream directed flow occurs (Figure 3b) and the shear layer reattaches to the inner bank (Figure 3d), implying that the zone of recirculation is spatially constrained and closed, opposed to the first stage, where the shear layer does not reattach to the bank (Blanckaert, 2018).

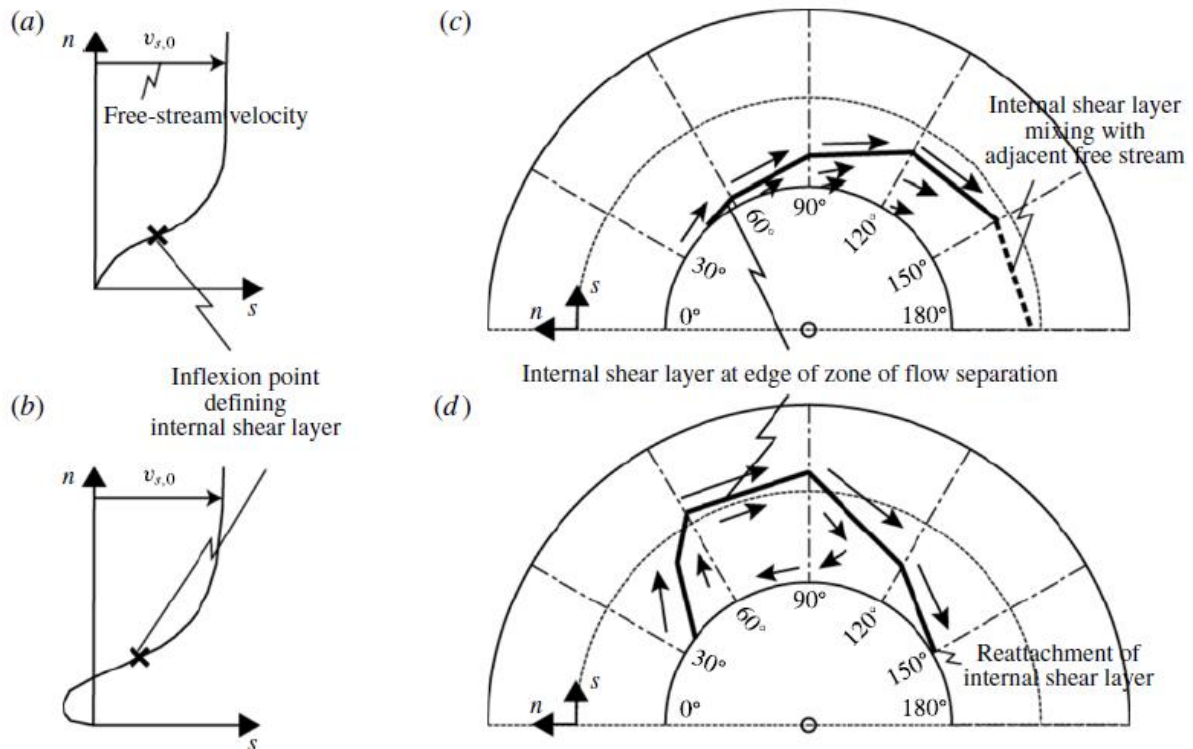


Figure 3:(a,b) Definition sketch of two stages of flow separation in a two-dimensional boundary layer. The zone of flow separation is delimited by an internal shear layer, which location is defined by an inflection point in the velocity profile. In the first stage, the velocity profile develops a deficit characterised by an 'S shape', but velocities remain downstream oriented. The internal shear layer weakens in downstream direction and mixes with the adjacent free flow. In the second stage, flow reversal occurs, and a recirculation eddy develops in the separation zone. The internal shear layer reattaches at the boundary. (c,d) First and second stage of flow separation at the convex bank in an open channel bend. (From Blanckaert, 2015)

Several processes are found to play a role in the beginning stages of flow separation. Firstly, when bend curvature increases, flow tends to follow a straight line away from the bed due to the inertial forces, particularly the centrifugal force. In the outer bend mass then accumulates, increasing the water surface elevation, and an inward pressure gradient is created by the difference in surface water elevation between the outer and inner bend. This inward pressure gradient opposes the inertial forces and steers the water back into the corner. This pressure gradient spatially lags behind the inertial forces, which plays a major role in promoting flow separation (Blanckaert, 2015). Along with this process, an adverse pressure gradient is formed in the inner bend due to lower flow velocities. Flow velocity increase reduces pressure, therefore the pressure created in the inner bend by the lower flow velocities will counteract the flow and may lead to flow reversal (Kleinhans et al., 2023).

These processes alone, however, are not sufficient conditions to explain the initiation of flow separation as shown by laboratory experiments by Blanckaert et al. (2013). Blanckaert (2015) describes three additional factors playing a role in the development of flow separation. Apart from the pressure gradients described above, the decrease in water surface elevation in the inner bend creates a streamwise water surface gradient in the upstream half of the bend, which accelerates flow at the inner bend. This accelerated flow opposes flow separation. Furthermore, a secondary flow cell that covers the entire width of the river bend is induced by bend curvature, which causes a helical motion with outward flow at the upper part of the water column and inward at the lower part. In the upper part of the water column, this induces flow separation, and in the lower part opposes flow separation. This is why the width of the separated flow area is largest at the water surface and decreases with depth, as shown by

Blanckaert (2015). Finally, a turbulence-induced flow cell develops near the inner bank, with velocities promoting flow separation in the upper water column, and velocities opposing flow separation in the lower water column (Figure 4H).

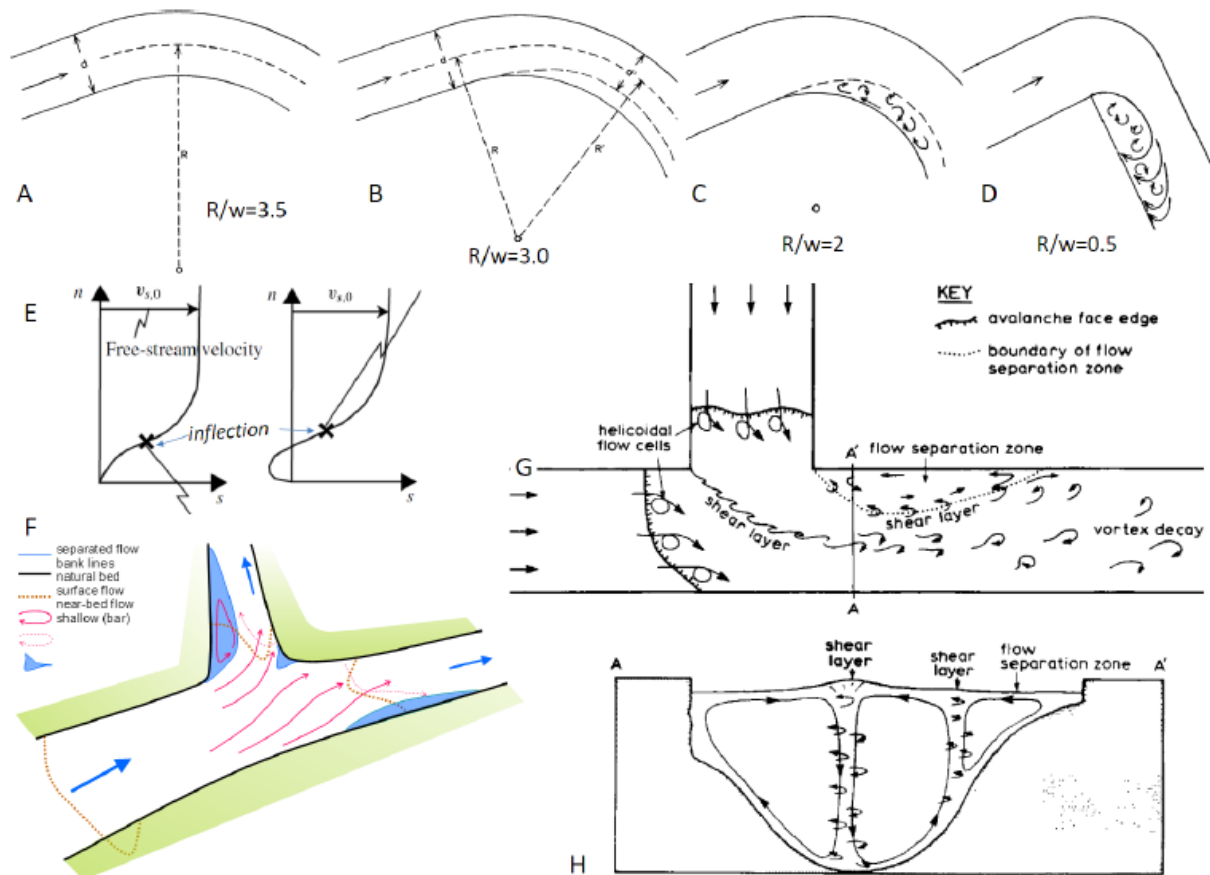


Figure 4: (from Kleinhans et al., 2023). Sketches of flow separation. A-D. Onset of flow separation and recirculation in increasingly sharper bends (Bagnold, 1960b). E. Horizontal streamwise velocity profiles plotted in streamwise (s) and normal (n) flow direction space, showing an inflection point between main flow and separated (left) and recirculation (right) zones (Blanckaert, 2015, see Figure 3). F. Presence of flow separation and recirculation zones in a bifurcation (Kleinhans2013). G,H. Plan view and cross-section of flow separation, recirculation and free shear layers at a confluence (best1986).

1.2 Effects of morphology on flow separation

The aforementioned factors contribute to the conditions that determine whether flow separation will occur, and with what intensity flow recirculation may take place. As the shape of the bend and bed is clearly a factor of crucial importance, the hydro-sedimentological processes and feedback deserve attention. This is underlined by Blanckaert (2010, 2015), who observed in laboratory experiments that with immobile bed experiments separation of flow occurred without second stage recirculation, while recirculation did occur in a mobile-bed experiment. As recirculation is also commonly observed in natural meanders (e.g. Leeder and Bridges, 1975; Ferguson et al., 2003; Vermeulen et al., 2015), this indicates that sedimentary and morphological processes play a major role in the development and working of flow separations. These processes and their influence on flow separation are not easily predicted nor modelled, and their effects in the Western Scheldt estuary are still to be researched. To be able to analyse the effects of hydro-morphological processes and interactions on flow separation in the Western Scheldt estuary, I will look at the relation between the location where the flow first separates and the morphology, which is influenced by the water depth. My first research question will therefore be: (1) What are the effects of the changing morphology caused by water elevation changes on the location where flow separates?

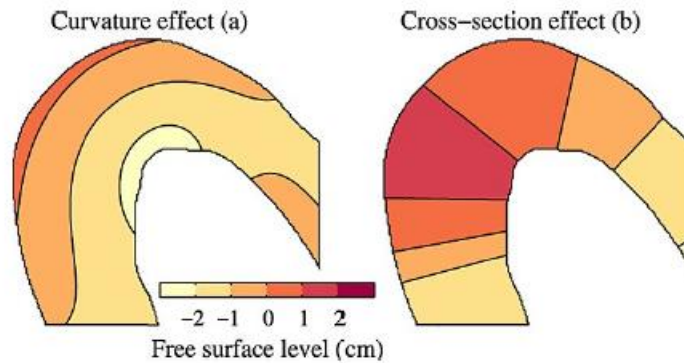


Figure 5: Water surface topography induced by curvature effects (a) and cross-sectional effects (b). Flow is from left to right. Curvature-induced pressure is on the upstream outer bank and downstream inner bank (a) while cross-sectional area-induced adverse pressure is located over the entire width, upstream of the largest cross-sectional area.

Experiments and observations show that channel curvature (Figure 5 (a)) can cause flow separation at the inside of bends, which is observed at sharp channel bends in both rivers and tidal channels (e.g. Leeder and Bridges, 1975). Alongside several dominant geometry parameters controlling flow separation, Blanckaert (2015) proposed R/w , where R is the minimum radius of curvature along the channel. Apart from the radius of curvature R , the width w is important as a larger w leads to larger lateral variation in depth-averaged velocity and a stronger adverse pressure gradient near the inner bank that leads to flow separation (Bo and Ralston, 2020). A decrease in R/w therefore results in a stronger separation of flow. This relation was already found in laboratory experiments by James et al. (2001) and in numerical models by Bo and Ralston (2020). The typical range of R/w found in rivers is 1.5 to 4.3, and in tidal channels 1.6 to 5, with very sharp meanders having values of 0.6 in rivers (Nanson, 2010) and tidal meanders 0.5 near sharp bend apexes (Marani et al., 2002).

Bo and Ralston (2020) observed flow separation using relatively low Froude numbers between 0.1 and 0.2 around R/w of 0.7-1.3. Their theoretical model suggests that flow separation shows dependence on shallowness and R/w and predicts conditions for flow separation to happen between $R/w < 1$ for “shallow” channels and $R/w < 1.5$ for “deep” channels. The shallowness of the channels was defined by the water depth over the along-channel bend length. H/L of $\sim 0.003 - 0.005$ was defined as shallow, H/L of $\sim 0.005-0.01$ as deep. Observing curved circular pipes, Bagnold (1960b) found the first stage of flow separation to begin at values of approximately $R/w < 3$, and the second stage begins at values of approximately $R/w < 2$. As the relationship between R/w and flow separation is still not well established and the values found in models do not accurately translate to real life situations, a next research question arises: (2) What is the relation between bend curvature and width (R/w) and flow separation in the Western Scheldt estuary?

Because of the role of inertia in the development of flow separation, Leeder and Bridges (1975) predicted flow separation as a function of R/w and the Froude number Fr . Bo and Ralston (2020) used low Froude numbers in their experiments, and Froude numbers in estuaries are typically low, but this raises an empirical research question: (3) what effects do changes in the Froude number have on the magnitude and width of flow separation zones in the Western Scheldt estuary?

Furthermore, as the turbulence induced secondary flow cell at the inner bend promotes flow separation at the upper part of the water column, the Reynolds number can be expected to be of importance for flow separation as well. The secondary flow induced by turbulence is conditioned by the production rate of turbulent kinetic energy, which depends on the accurate

description of the Reynold stresses (Blanckaert, 2015). When Reynold numbers increase, the mixing of momentum into the boundary layer will also increase, since the turbulent viscosity is much larger than the molecular viscosity. As a result the location where the mean flow separates from the bank moves downstream, and the recirculation area is compressed (Kleinhans et al., 2023). Surface roughness can also enhance the mixing of momentum, thereby moving the point of flow separation downstream. In other words, lower Reynolds numbers will lead to a larger and more defined zone of flow separation. As Reynolds numbers in estuaries are typically high, the question remains how large a role these Reynolds numbers will play. This leads to the fourth research question: (4) What is the relationship between Reynolds numbers and flow separation in the Western Scheldt estuary? Here, factors that influence viscosity and thereby Reynolds numbers such as water temperature, salinity and sediment load are neglected.

Processes favouring the onset of flow separation can also originate in hydro-sedimentological interactions. In sharp corners, a transverse bed and a deposition bar typically develop at the inner bank. These morphological features favour flow separation as they cause an outwards velocity redistribution due to topographical steering (Blanckaert, 2018). Positive feedbacks between flow and sedimentological processes lead to a widening of the zone of flow separation or recirculation as observed by Blanckaert (2010, 2015). In time this can lead to the second stage of separation which includes recirculation, which again causes sedimentation leading to a wider zone of flow separation up unto the point that the sedimentation zone rises above the water level. The turbulence-induced secondary flow cell near the inner bank depends on the roughness, inclination and shallowness of the bank. Flow separation can therefore be expected to be promoted near rougher, shallower banks. This leads to the final research questions: (5) What are the effects of bank roughness on flow separation in the Western Scheldt estuary? And (6) How does water depth affect the magnitude and shape of the flow separation zone in the Western Scheldt estuary?

1.3 Research questions

The following problems arise from the literature review. The effects of the combination of processes and mechanisms are not well understood in a real life setting. Therefore, empirical research is needed to give insight into the phenomenon of flow separation in the Western Scheldt estuary. Due to the importance of the estuary as a shipping lane, understanding of these factors is eminent, but it is still not clear under which conditions flow separation develops. The aim of this thesis was therefore to empirically determine the hydro-morphological factors determining the point where flow separates in sharp corners of the Western Scheldt estuary, and properties of the flow separation zone in relation to the tidal phase and the morphology of the bed and bars. To this end, I found the following research questions:

- (1) What are the effects of the changing morphology caused by water elevation changes on the location where flow separates?
- (2) What is the relation between bend curvature and width (R/w) and flow separation in the Western Scheldt estuary?
- (3) What effects do changes in the Froude number have on the magnitude and width of flow separation zones in the Western Scheldt estuary?
- (4) What is the relationship between Reynolds numbers and flow separation in the Western Scheldt estuary?
- (5) What are the effects of bank roughness on flow separation in the Western Scheldt estuary?
- (6) How does water depth affect the magnitude and shape of the flow separation zone in the Western Scheldt estuary?

Based on the literature, the following hypotheses were formulated:

- (1) It is to be expected that positive hydro-morphological feedback processes will promote flow separation as deceleration of the flow will increase sedimentation and the following shallowing of the region will further decelerate flow, increasing flow separation.
- (2) With smaller values of R/w , meaning smaller radii and larger channel widths, flow separation will be stronger
- (3) With lower Froude numbers, flow separation is expected to be stronger.
- (4) Lower Reynolds number are expected to lead to stronger and more expressed flow separation in the Western Scheldt.
- (5) Increased bank roughness is expected to slow down near-bank flow and therefore promote the second stage of flow separation.
- (6) Shallowness in the inner bend is expected to promote flow separation as flow slows down flow. A strong inclination of the bed is expected to increase a velocity gradient and thereby promote flow separation.

2. Methods

In this thesis, I use satellite images combined with GIS to identify flow separation zones and analyse the found regions by pattern and flow velocity model data. The images are taken from different moments in the tidal cycle to be able to analyse the same morphology over different water levels and hence water depths and flow velocities.

For this study, the satellite images are collected from planet and satellietdataportaal.nl (Planet Team, 2023; Satellietdataportaal.nl, Netherlands Space Office, 2023). The locations where flow separation occurs can be observed by noting differences in suspended sediment load (Figure 6). The determined points of separation are compared over a tidal cycle.



Figure 6: Sediment concentration at the water surface of the Westerschelde, showing indications in sediment concentration visible at the water surface for flow separation on the eastern side of the large bar. In orange the location of Figure 15 a) Image: 2023-05-31 planet imagery “Imagery © 2023 Planet Labs”.

2.1 Used imagery

The Planet images are PSScene orthorectified, colour-corrected RGB imagery, with a resolution of 3m. The images from satellietdataportaal.nl are Pléiades Neo and have a resolution of 0.3m. To be able to analyse images over an entire spring-neap cycle, the Planet images were used. These images were taken daily at similar times, and could thus be used to visualise the tidal cycle as high water peaks shift daily. The imagery resolution determines the resolution at which the shear layers could be observed. The scarce availability of the high-resolution images from satellietdataportaal.nl limit the practical application of these images for analysing an entire tidal cycle. Only three suitable images that coincide with the study area were available (NSO in Table 1), which is not enough to observe changes over the tidal cycle. These images were therefore used alongside the Planet images to observe the area of interest more closely.

Table 1: An overview of the selected dates and times corresponding to the used images. The green sources represent good quality images, and the yellow sources images of worse quality. The times shown are in GMT+1, while the water elevations at Hansweert are in NAP (Normaal Amsterdams Peil), the Dutch mean sea-level standard. NSO (Netherlands Space Office) represents the images from satellietdataportaal, and planet the Planet images.

source	date	time	tidal phase	HW Hansweert	elevation HW (NAP)	time LW Hansweert	elevation LW (NAP)	elevation Hansweert
planet	2023/06/16	10:18	flood	13:48	250	7:44	-225	-73
NSO		10:46	flood					-39
planet	2023/06/15	9:52	flood	12:56	246	6:55	-227	-44
planet	2023/06/14	9:52	flood	12:00	238	5:58	-224	65
planet	2023/06/13	10:18	flood	10:58	230	4:48	-222	213
planet	2023/06/11	9:47 +	ebb	8:42	235	14:54	-169	197
		9:54						
planet	2023/06/10	10:42	ebb	7:37	245	13:50	-179	42
planet	2023/06/08	10:25	ebb	5:32	270	12:04	-202	-110
planet	2023/06/07	9:48	ebb	4:42	279	11:18	-211	-130
planet	2023/06/06	9:49	ebb	16:23	265	10:33	-219	-191
NSO		10:53	flood					-212
planet	2023/06/05	9:55	LW	15:40	273	9:50	-224	-224
planet	2023/06/04	9:51	flood	14:59	277	9:07	-227	-198
planet	2023/06/03	10:26	flood	14:20	274	8:25	-226	-106
planet	2023/06/01	9:53 +	flood	12:59	244	6:55	-210	-27 + -37
		9:46						
NSO		10:57	flood					82
planet	2023/05/31	9:47	flood	12:14	218	6:02	-196	47

2.2 Used data

The period of interest is based on the availability of clean images (Table 1). A mostly uninterrupted series of cloudless images over a period of approximately two weeks is needed to cover the entire spring-neap tidal cycle of a semidiurnal tidal system.

The mean discharge of the Scheldt river is about $120\text{m}^3/\text{s}$ $5 \times 10^6\text{m}^3$ per semi-diurnal tide (Wang et al., 1999). This is less than 1% of the tidal prism of about $2 \times 10^9\text{m}^3$. The main forcing mechanism in the estuary is thus tidal. Additionally, in spring, during the period of interest, river discharge was relatively constant (Figure 8), so it is reasonable to assume that there are no measurable effects of discharge variation in the researched period. Furthermore, small morphological changes are neglectable. With these assumptions the images between multiple and different tidal cycles can be compared.

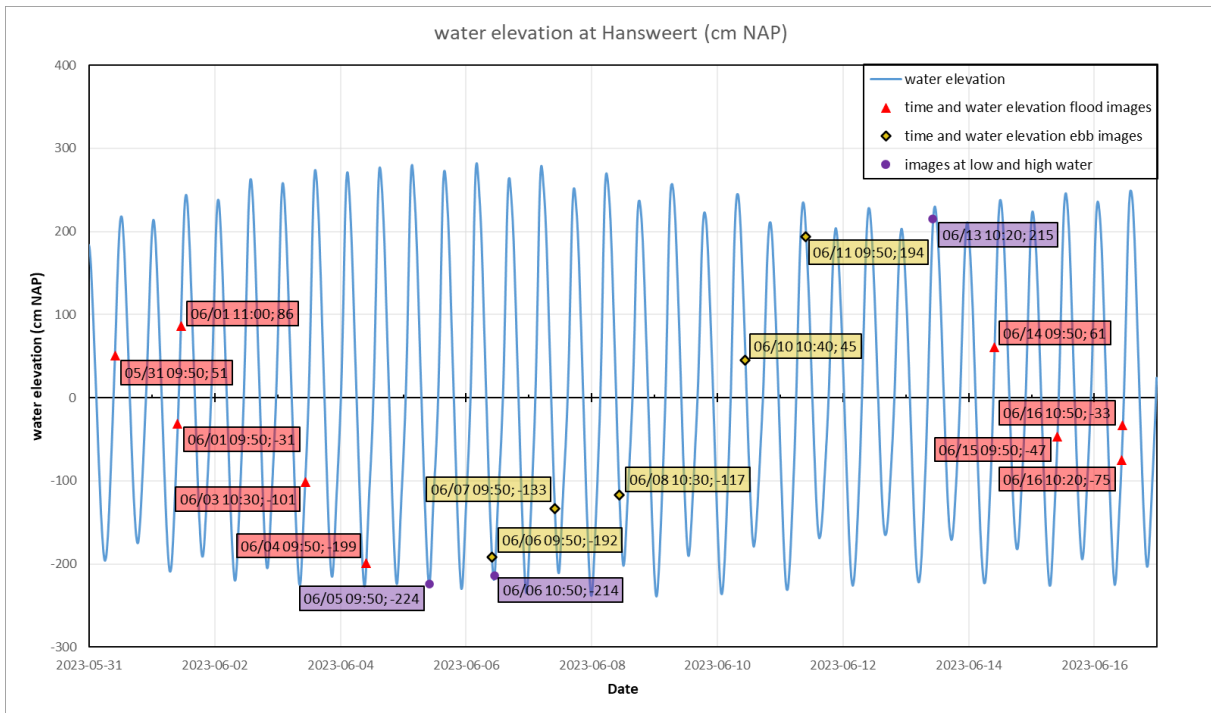


Figure 7: Water elevations of the images used in this research in cm NAP. Images taken during flood are in red, images taken during ebb are shown in yellow, and high water and low water images are shown in purple.

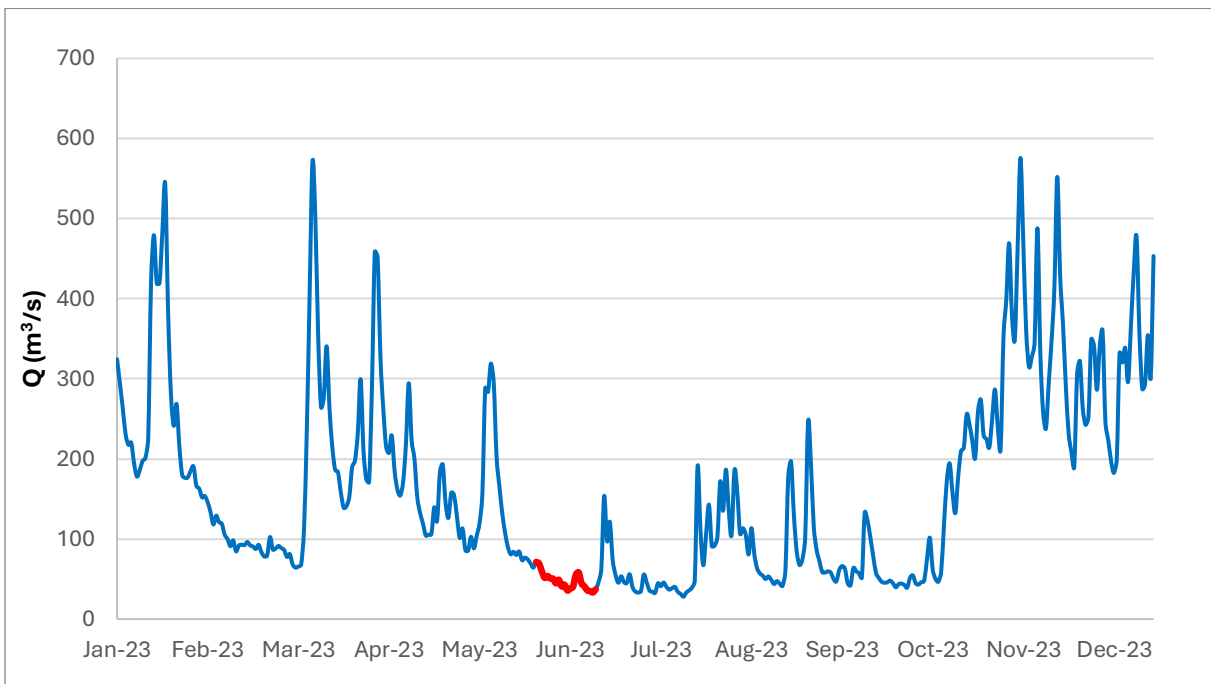


Figure 8: Discharge [Q] of the Western Scheldt at the Belgian-Dutch border. In red the period of interest. Data of Flanders Hydraulics, a division of the department of Mobility and Public Works of the Government of Flanders on waterinfo.be.

The region of interest is located around the Ossensisse shoal (Figure 1), which has been subject to previous research due to its complex flow patterns (Plancke et al., 2020). The region has been chosen after a preliminary analysis, which showed that the most prominent and constant flow separation zone is located around the apex of the Ossensisse shoal.

I used ArcGIS to highlight the turbulent shear layers that were visible on the satellite images as well as sharp boundaries between bodies of water with a different colour. This colour difference indicates a different sediment concentration, which can be caused by different flow velocities separated by a boundary layer. These regions thus could be interpreted as flow separation zones, which are at their widest at the surface (see Blanckaert (2015) and chapter 1.1). I then combined the different highlighted lines and zones into one Figure (Figure 10, 11), to find patterns, and colour coded lines in (Figure 14, 16) to see how the separation zones change with different water levels. To further analyse the data, I compared the found locations with a 2DH Waqua model scalwest 2000 provided by *Rijkswaterstaat Zee en Delta*, which used measured hydro-meteo conditions on the boundaries and the bathymetry of 2023. This bathymetry was also used to analyse the effects of water depth (shallowness) to flow separation.

Not every one of the hypotheses derived from the literature review can be tested as there is not sufficient data available. The bank roughness and the bed roughness could not be quantified for the Western Scheldt with the resources available. Instead, the focus will be on the radius to width ratio and the shallowness of the flow defined by the tidal phase, and an occasional observation of bedforms. The morphology will be used to predict the locations at which flow separation will occur, and the tidal phase will be used to observe difference in flow separation magnitude and width, additional to shifts upstream or downstream in location. To determine the effects of water depth, I used the bathymetry of 2023 provided by Rijkswaterstaat combined with local water elevation measurements from the model and local measuring stations. To determine R/w , I used ArcGIS to draw circles fitting the bend at that location over a length of approximately 2000 metres. The length the curvature was relatively constant for the three locations that were used (Figure 19). The circles provided a radius, and the widths were measured in ArcGIS.

For the Froude numbers and the Reynold's numbers, flow velocities from the model were used. The Reynold's numbers could be calculated by using the formula:

$$Re = \frac{u_{avg} * R_h * \rho}{\nu} \quad (1)$$

Herein, u_{avg} is the average flow velocity in m/s over the width of the estuary at a fixed location near the Ossensisse shoal (Figure 20), R_h the hydraulic radius in metres, taken as a measure for the characteristic length, ρ the water density of 1010 kg/m^3 , and ν the dynamic viscosity of $1.2 \times 10^{-6} \text{ kg/m} \cdot \text{s}$. The hydraulic radius R_h is calculated by dividing the cross-sectional flow area (A in m^2) by the wetted perimeter (P_w in m). Because the estuary is much wider than it is deep, the area could be approached to be $h * w$ where h is the water depth and w the width of the estuary, and the wetted perimeter could be approached to be $P_w = 2h + w$, leading to the formula:

$$R_h = \frac{h * w}{2h + w} \quad (2)$$

3. Results

The observed flow separation zones are predominantly attached to the banks, as is visible in Figure 9. For clarity, the separation zones will not be shown as zones, but rather only the shear zone (a layer observed as a line at the surface) will be shown from now on.

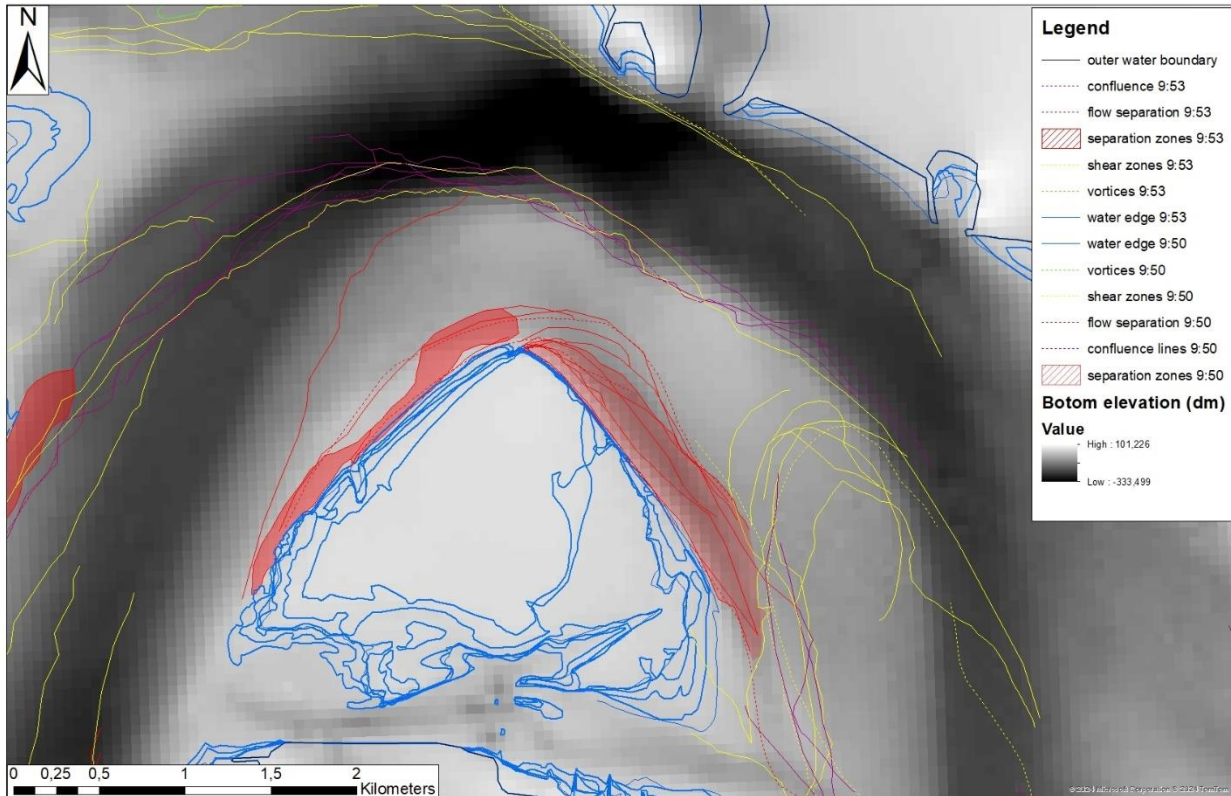


Figure 9: Collected observations of separation zones, shear zones and depth during different moments of the flood tidal cycle around the ridge of Baarland and the Ossenisse shoal over the bathymetry.

3.1 Trends and observations

In Figure 10, all observed shear zones for flood are portrayed in one image. There are a few trends that can be deduced from this image. Firstly, it is clear these images were all taken during the flood phase, as all portrayed lines have an inland direction, starting to the west and continuing east. This shows that the found tidal phase is in line with the tidal phase of the taken images. Secondly, many of the found shear zones are located at the edge of the main channel. This is not only the case for lines that were interpreted to be part of a separation zone, but also for a channel confluence and other shear zones. The main channel is used by both flood and ebb currents, and it is the main sailing route for the large container ships heading for the Antwerp harbour. The adjacent channel is frequently dredged, as is agreed upon by the Belgian and Dutch governments, to make sure the Antwerp harbour will continue to be accessible for cargo ships. The reason the lines are located at the edges of the main channel, is because there is a large mass of fast flowing water through the main channel, while the water flowing over the shallower parts will have a much lower flow velocity. This results in turbulence at the border of the two bodies of water, shown as small-scale irregularities the shear zones and vortices that can be seen in Figure 10.

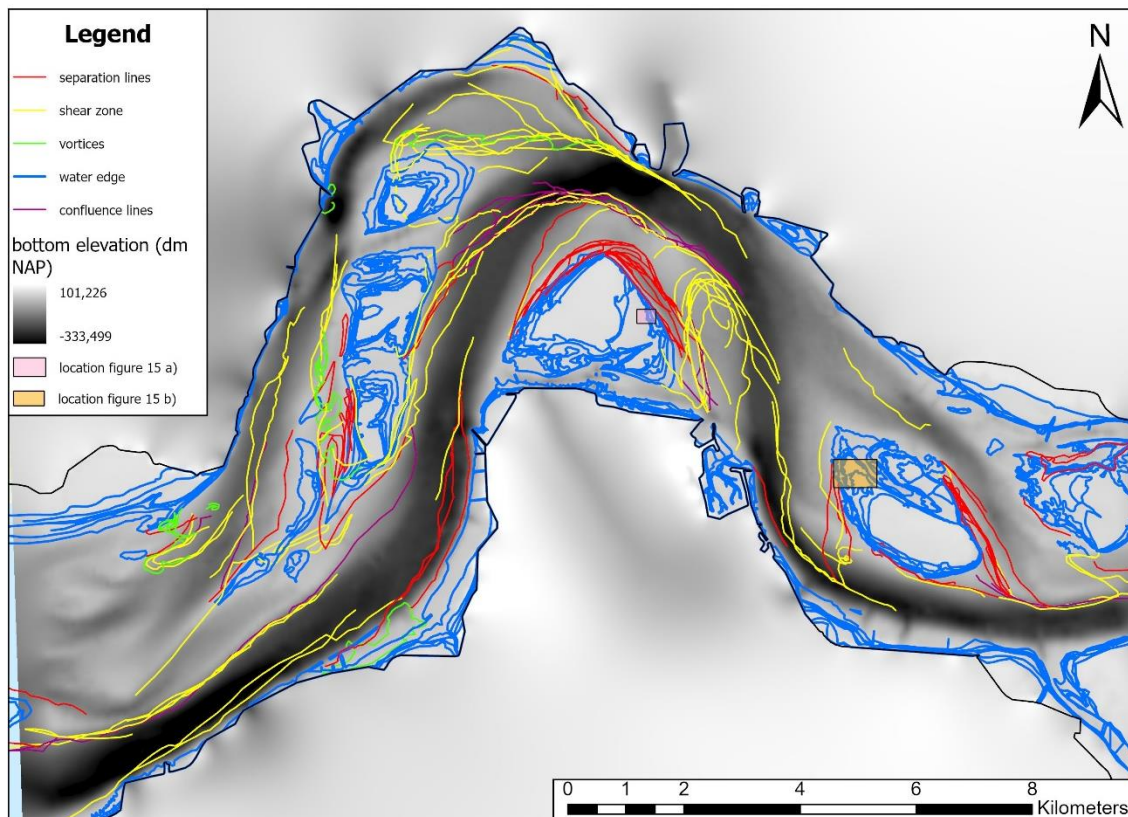


Figure 10: Observed shear zones during different moments of the **flood** tidal cycle in the Western Scheldt over the bathymetry (with the water edge or water line of these moments drawn in blue). Boxes in pink and orange indicate the locations of Figure 15, that show megaripples.

Interestingly, many shear zones appear in the flood phase right behind a protrusion or sharp corner in a bar or at the banks. This happens at several locations at the ridge of Baarland, the Ossenisse shoal, and the shoal of Walsoorden. These shear zones do not cross the main channel, and mostly, a difference in sediment concentration can be observed to either side of the shear zone. I have given these shear zones a red colour, to indicate my interpretation of these zones to be the result of flow separation. Around the Ossenisse shoal, there is a subtidal shallow plateau bordered by the main channel flowing around it. Directly east of the shoal, where shear zones were observed throughout the flood tidal cycle, there is a deeper elongated section or channel, better visible in Figure 11. Finally, Figure 10 shows a lot of shear zones east of the Ossenisse shoal in yellow, which indicate a strong turbulent region. This region will be discussed in chapter 3.1 and 4.1.

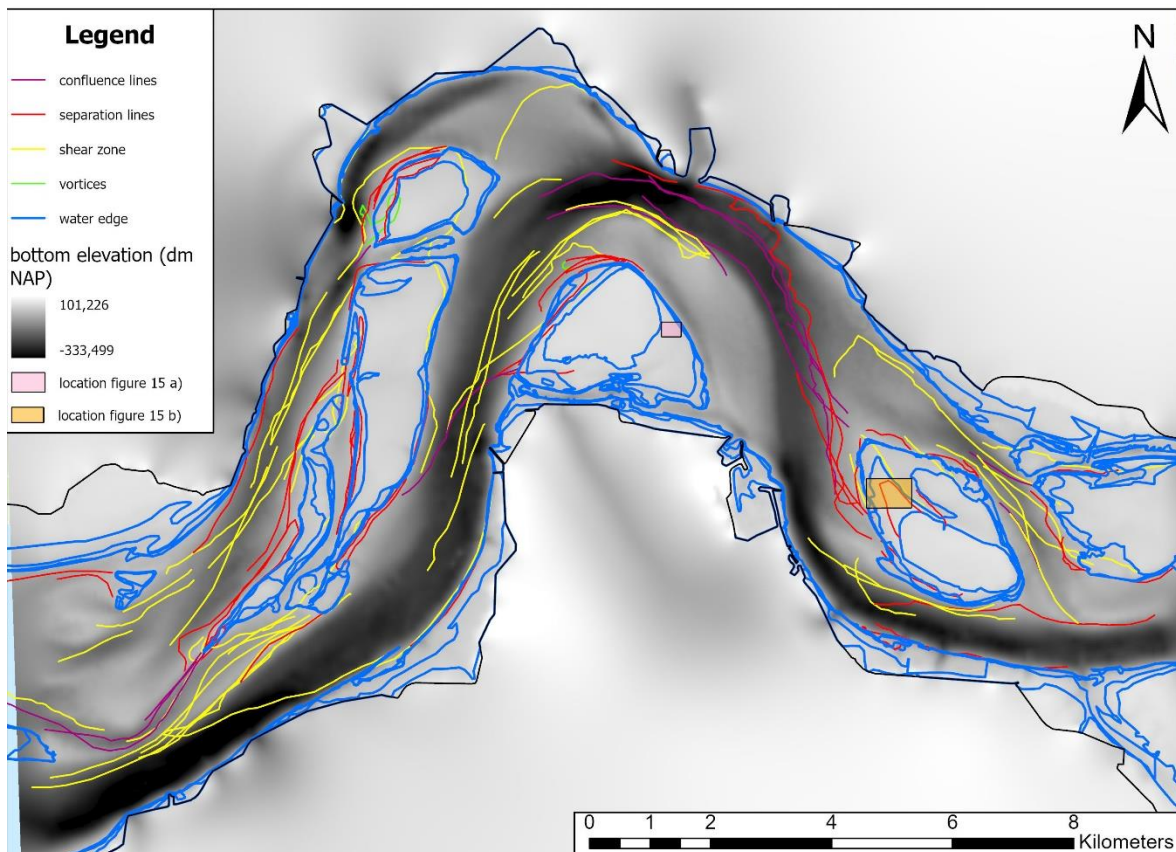


Figure 11: Observed flow separation zones and shear zones and depth during different moments of the **ebb** tidal cycle around the ridge of Baarland and the Ossensisse shoal over the bathymetry (see Fig. 10).

Figure 11 shows the same image, but only the lines drawn over images of the ebb tidal phase are shown. Less images of adequate quality were found during the ebb phase, which is why there are less lines shown. During ebb, similar to during flood, many shear zones are hugging the edges of the main channel. While the separation zones are again located next to the bars and banks, many start in different places from the flood separation zones, with the apex of the Ossensisse shoal as an exception. This shows that this location is of interest for the understanding of flow separation.

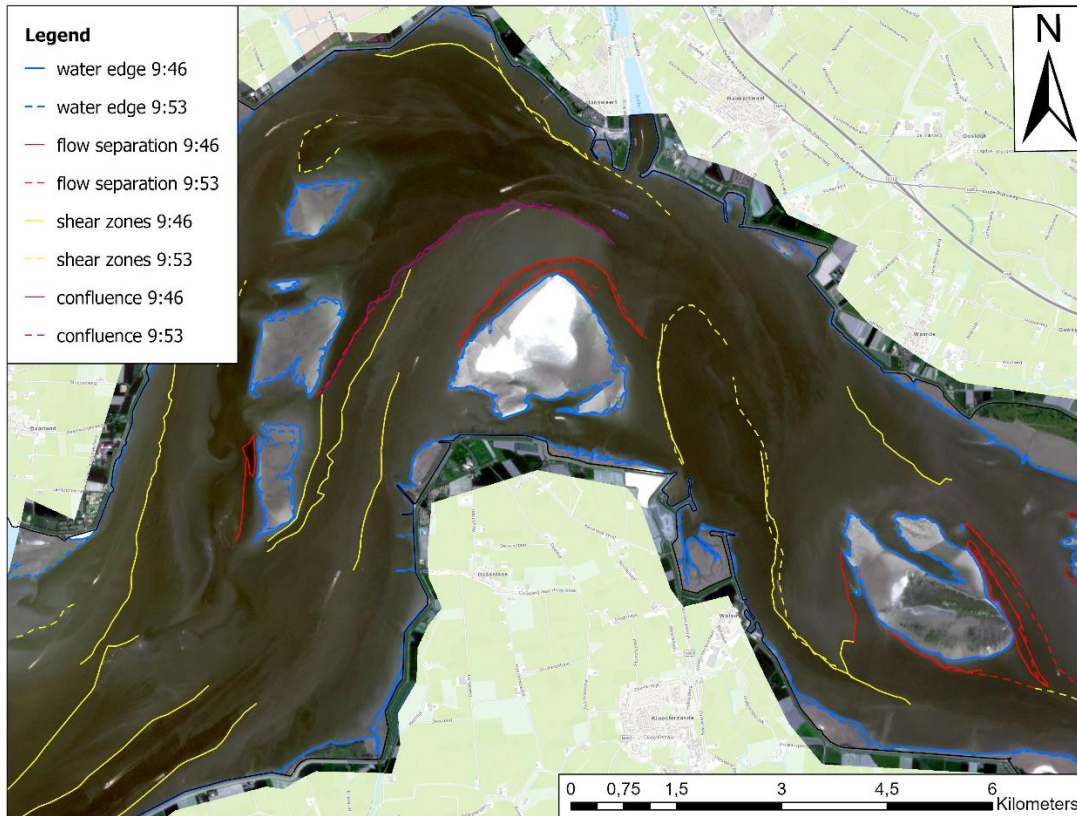


Figure 12: Flow separation in flood flow in the Western Scheldt at 2023/06/01 at 9:46 (solid lines) and 9:53 (dashed lines) on the satellite image from 9:46.

To test whether the interpretations of the shear lines are repeatable, two different sets of lines are shown that were based on images taken 7 minutes apart (Figure 12). The majority of shear zones could be traced around the same place at both times, which shows that the found locations are quite stable, and the research is reproducible. Interesting areas in the image are similar to the locations found in Figure 10, but additional observations arise from Figure 12. Over and along the ridge of Baarland there is much turbulence where the bar is flooded. A sediment-poor flow is located west, with large turbulent eddies clearly visible at the left side of the area (Figure 13). The upstream (south) part of the area is rounded, which can be explained by the presence of an underwater bar. In Figure 13 b), the low water image shows that there is indeed a bar located there, causing this sediment-poor region. These kinds of regions show that inner bend flow separation is not the only kind of flow separation that occurs in the Western Scheldt, but that separation of flow can also occur due to the existence of intertidal bars and is in fact ubiquitous.

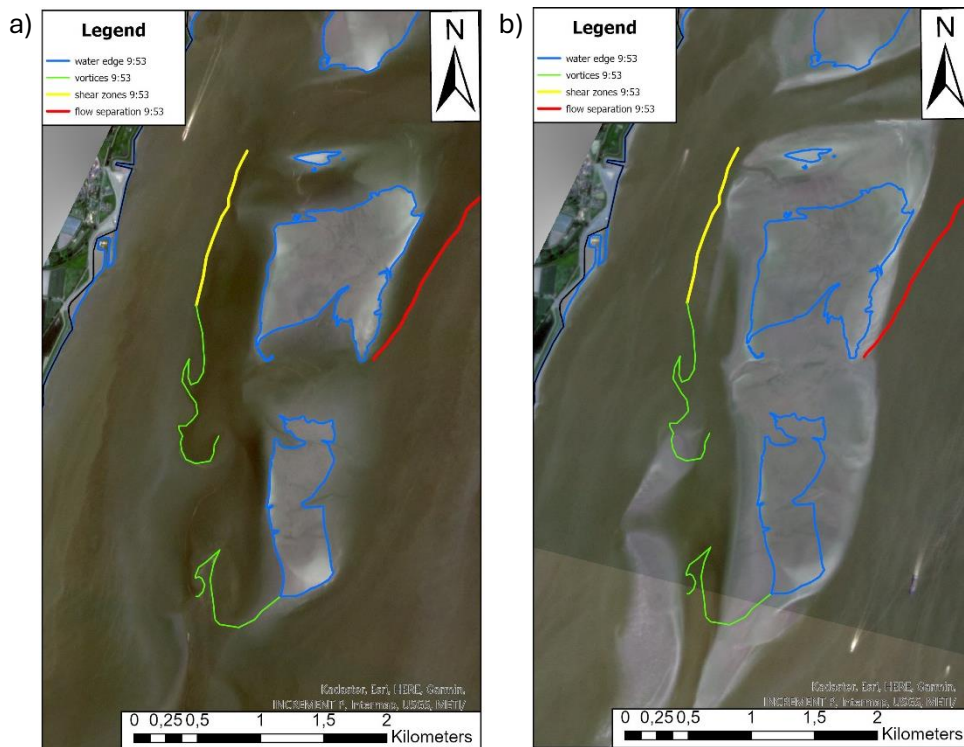


Figure 13: Figure 11 zoomed in on the ridge of Baarland with satellite images of a) 09:53 at 2023/06/01 with a water level of -27cm NAP and b) the same observations superimposed on the satellite image of 10:30 at 2023/06/05 at low water (-214cm NAP).

3.2 Influence of changes in water depth

In Figure 14, a sequence of flow separation zones that correspond with different moments in the tidal phase is shown. Several trends are noticeable. First, with rising water level, the flow separation zone enlarges. The smallest zone in yellow, corresponds to a water level of -199cm NAP (also Table 1, Figure 7) and is also the shortest. This indicates that the separated flow at this time is the weakest and might not even be recirculating. Comparing Figure 7 and comparing the moment in the tidal cycle with the flow velocities in the model (Figure 17), it is to be expected that flow velocities near the bar are still not very high as it is only 44 minutes after low water (Table 1). At -101cm NAP, the separation zone is wider, and continues further downstream, and this trend continues with the +51 and +61cm NAP zones. The -27 and -47cm NAP separation zones, seem to deviate from this trend slightly, as they are not as wide as the -101cm zone. However, they are still wider than the -199cm NAP line, and appear to become wider still than the -101cm NAP line downstream.

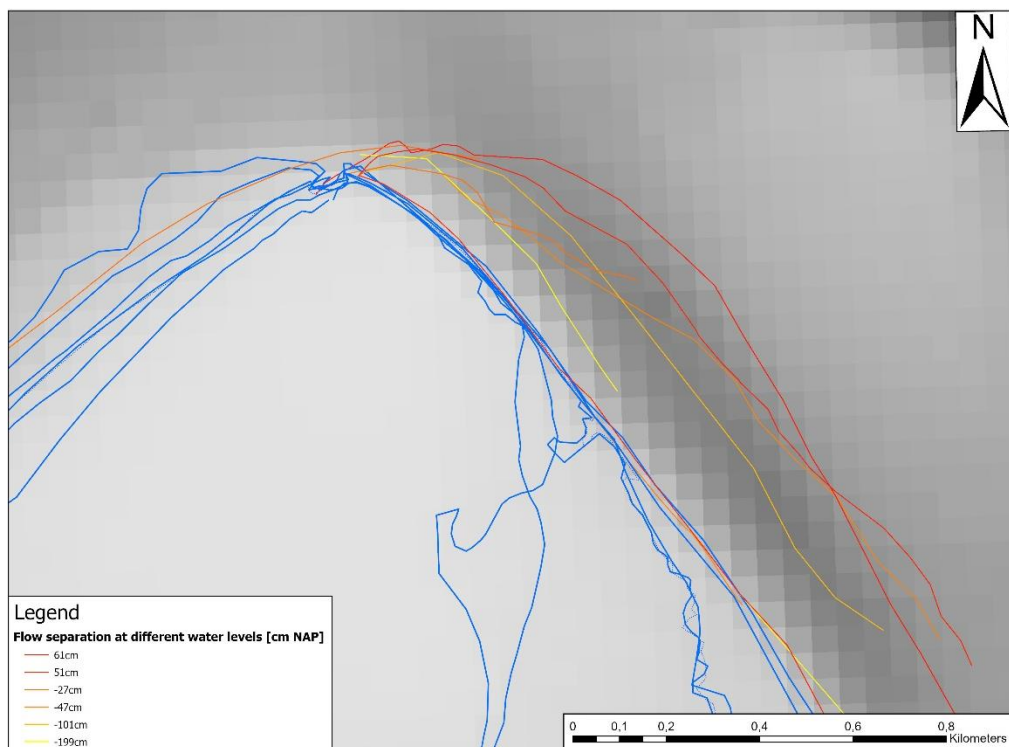


Figure 14: From yellow to red: the observed separation zones with rising water levels during flood around the apex of the Ossenisse shoal

Another trend that can be observed is that the widest part of the separation zone tends to shift downstream with higher water levels. With such consistent separation zones at this location, it can be expected that the second stage of flow separation (Blanckaert, 2018) is reached, which is supported by evidence of the presence of ebb-dominated flow ripples (Figure 15a). Here, the main direction of flow can be observed to be in ebb-direction, which suggests that there is no strong flood current at this location. The emergent ebb-dominant megaripples are not common in the Western Scheldt estuary because ebb water levels are generally lower, but in zones with flow circulation they appear to exist in at least two locations, as in Figure 15b, with flood-dominant ripples on the north-east side of the shoal of Walsoorden.

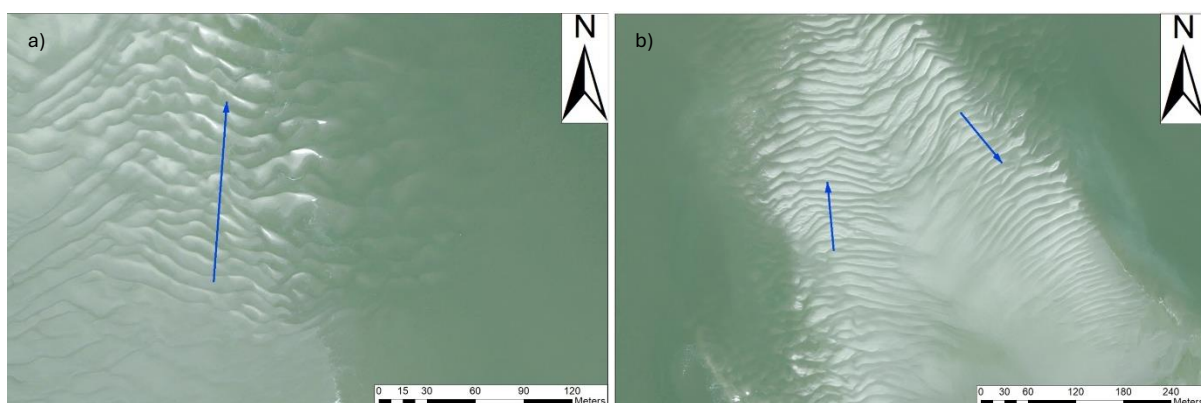


Figure 15: Mega ripples on a) the Ossenisse shoal and b) the shoal of Walsoorden. In blue the dominant flow direction based on megaripple orientation. The location of both images is shown in Figure 10 and 11.

East of the Ossenisse shoal, a cluster of shear zones can be seen in Figure 10. Throughout the tidal cycle, eddies and vortices can be observed at this location. Figure 16 shows that no clear trend can be seen over a tidal phase. With higher water levels, the zone is not consistently migrating a certain direction, or clearly widening. The shear zones are all located on a shallow part of the estuary, as shown by the bathymetry.

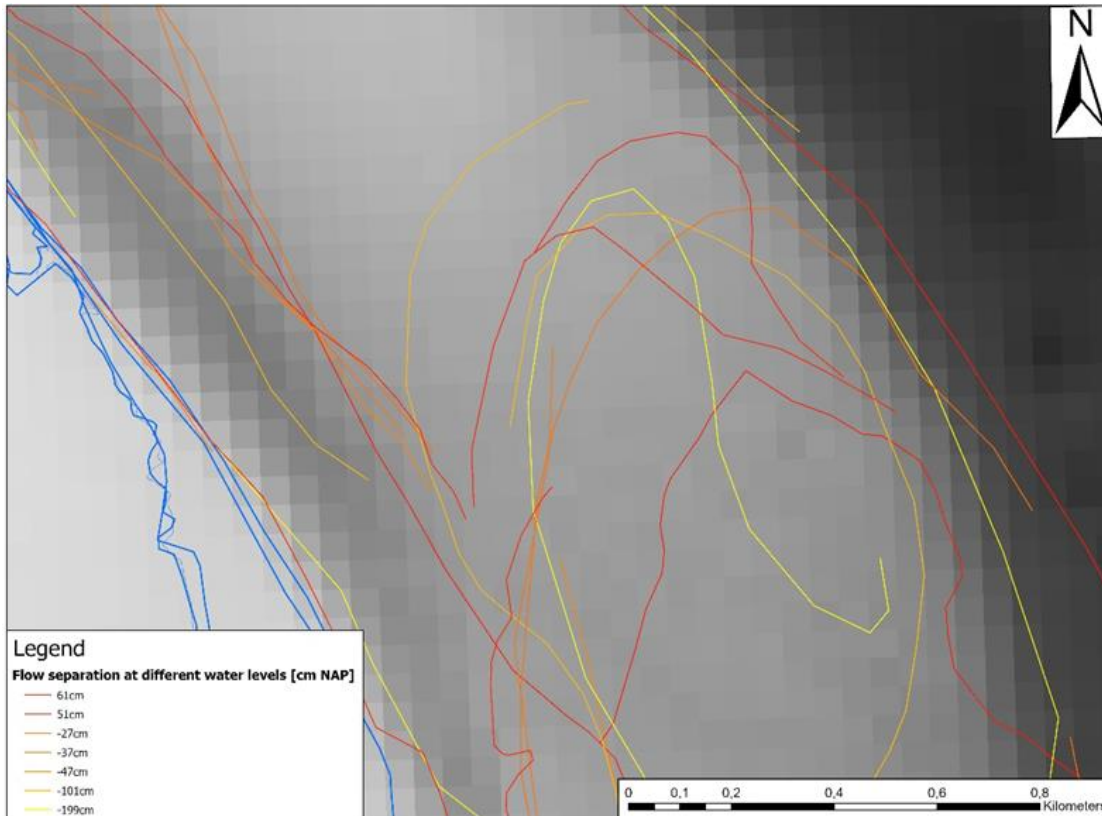


Figure 16: Shear layers east of the Ossensisse shoal over different heights in the tidal cycle in the flood phase. Yellow represents the lowest water levels, and red the highest. The lines to the left are the same as shown in Figure 14, and the lines bordering the darker region are lines alongside the main channel. In the middle of these two sets of lines, a cluster of squiggly lines represent the turbulent area over the shallows, which will be further elaborated on in Figure 18 and the discussion.

4. Discussion

Before the hypotheses can be addressed, there are still some observations to be interpreted. In Figure 10, some shear zones appear to be crossing the main channel in between the ridge of Baarland and the Ossenissee shoal. The turbulent layers that start in between the ridge of Baarland and the Brouwers shoal are most likely a result of two bodies of water combining, forming a confluence. As the two bodies of water come together, turbulent mixing will occur that shows as a shear layer that passes the main channel. These layers will therefore not be interpreted as flow separation. An observed shear zone in the middle of the channel right to the ridge of Baarland is most probably nothing more than the wake of a ship that has passed at that location. The wake of ships could be confused for a naturally occurring shear zone, but mostly, the found shear zones are located at the edge or even outside the main shipping channel, so the wakes of large ships are often not interfering with the research.

4.1 Ebb dominated channel and plateau bordering the Ossenissee shoal

The flow separation zones that develop around the apex of the Ossenissee shoal during flood are located over a channel on the shallow plateau surrounding the shoal, especially on the landward edge (Figures 11, 14). The ripples found on the shoal at low tide of Figure 15 a) suggest a strong current in the ebb direction. In the model (Figure 17), this region is shown as the first place where the ebb flow starts when the tide turns. My interpretation is that the separation of flow gives rise to a recirculating current, which coincides and amplifies early ebb flow. While the lower flow velocities that come with shallower waters lead to sedimentation all over the plateau, due to the early ebb-current, this channel will be eroded more than the surrounding morphology. This then is conducive to eroding the eastern side of the shoal, which maintains the triangular shape. The ebb dominated channel is thus a result of the separation of flow.

Next to this ebb-tidal channel, there is a shallower part of the plateau, where many shear zones could be observed (Figures 10, 16). Looking at the model (Figure 18), this area also has striking dynamics. At this location, the slower flow velocities don't continue in the same direction as they do at the surrounding areas and at multiple times, large eddies could be observed. The flow patterns have been known to be complex there for longer and Plancke et al. (2020) explained the measured flow patterns he used to validate 2 numerical models as follows: The tidal propagation over this sandflat during flood is relatively slow due to differences in bottom friction, which results in a water level reduction above the shoal. This leads to an adverse pressure gradient driving a return flow, which causes eddies when it comes in contact with the regular flow.

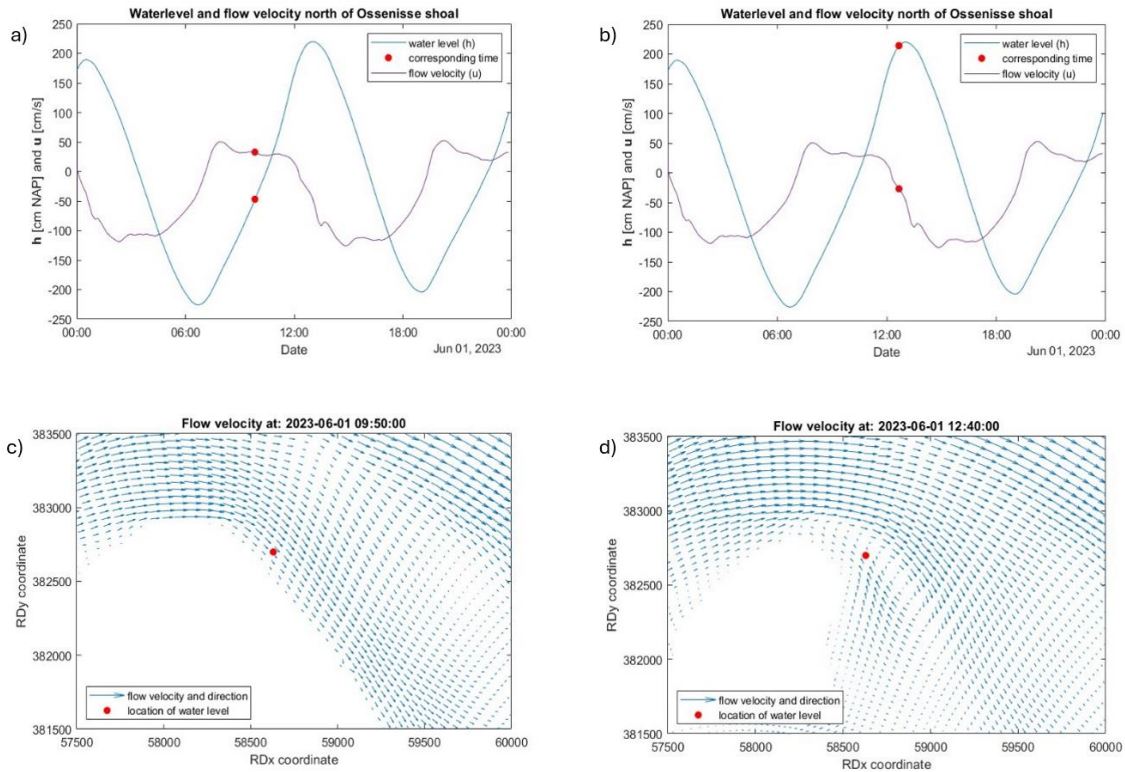


Figure 17: Output of the 2DH Waqua model scalwest 2000 provided by Rijkswaterstaat Zee en Delta. a) and c) Water levels (cm NAP) and flow velocities (cm/s) at the location shown in Figure b), d), north of the Ossensisse shoal. The sign of the flow velocity is based on the flow velocity in the x-axis, rather than the direction of the channel. A better impression of direction is given by Figures b) and d), where vectors showing the flow velocity are portrayed that correspond to the times of Figures a) and c), respectively. The time of 09:50 in Figures a) and c) corresponds with the observed image of 2023/06/01, also shown in Figure 12. b) and d) show the moment just before high water, where a return flow is already present east of the Ossensisse shoal, while the main current is still in flood direction.

Unsurprisingly, the model does not perfectly represent the flow conditions around the separation zone. During flood, where satellite images clearly show a boundary layer and separated flow, the model often does not show this in differences in flow velocity because it is a two-dimensional flow model without the required turbulence closure to obtain flow separation and shear zones. The model does however show that the ebb-flow starts at the same location where the flow separation occurs. As the separation zone decreases in width with depth (Blanckaert, 2015), the megaripples shown in Figure 15a) are most likely to be the result of the ebb flow rather than the recirculating flow during flood, which is still considered to have its observed flow pattern as a result of the recirculating current.

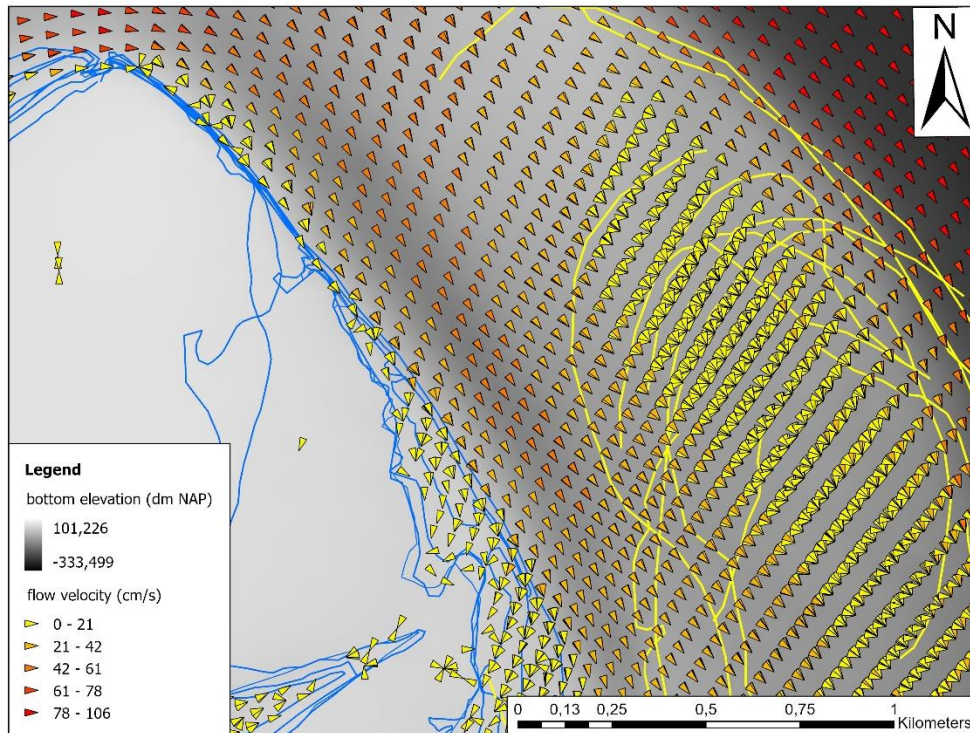


Figure 18: Flow velocity based on the model from Rijkswaterstaat, east of the Ossenisse shoal. In yellow the shear zones found at various water levels during flood. The red arrows in the main channel all have the same direction (with varying flow velocities), while the yellow arrows that coincide with the shear zones show a large range of directions.

4.2 Bend curvature

Literature suggests that the bend curvature R/w is an important factor to determine whether or not flow separation will take place (e.g. Bagnold, 1960b; Leeder and Bridges, 1975; Blanckaert et al., 2013; Bo and Ralston, 2020). In Figure 19 and Table 2, the values found in the Western Scheldt around the Ossenisse shoal are shown. When we calculate the R/w_c values with the width of the main channel (which neglects the multi-channel nature of the system), the sharpest section of the bend does not drop below the value of 1.5, which is found to be a threshold for flow separation in the “deep” channels with $H/L \sim 0.005-0.01$ (Bo and Ralston, 2020). The R/w_e value of 0.81 (Table 2), would satisfy the condition for both shallow and deep channels found by Bo and Ralston (2020). However, the flow is not limited to a single channel due to a shallow shoal separated from the bar by a channel and the concurrent asynchronous tidal reversal pattern. The presence of flow separation zones at locations other than the apex of the Ossenisse shoal shows that R/w is not a defining predictor for the occurrence of flow separation in the Western Scheldt estuary. The zones along the edges of the Ridge of Baarland and the shoal of Walsoorden (Figures 10 and 11) have corresponding bend radii that are notably much larger than around the Ossenisse shoal. They therefore do not satisfy the conditions given by Bo and Ralston (2020), ruling out R/w as a single defining factor.

Table 2: Bend radii and widths on the locations shown in Figure 12. R/w_c shows the R/w with channel widths, R/w_e the bend radii with estuary widths.

	Radius (m)	Width channel (m)	R/w_c	Width estuary (m)	R/w_e
1	1582	940	1.68	1962	0.81
2	3207	1062	3.02	2151	1.49
3	5053	1241	4.07	2876	1.76

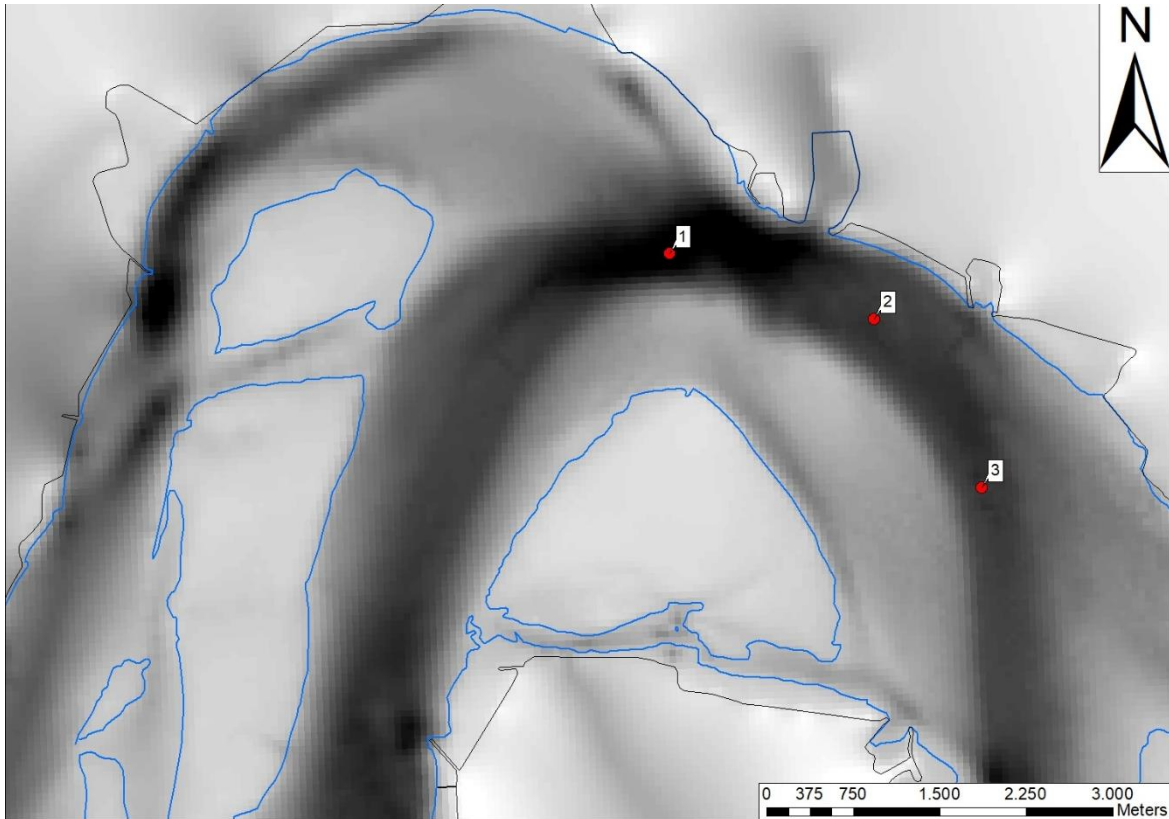


Figure 19: Locations of defined bend radii and widths as shown in Table 2.

4.3 Turbulence

Another factor mentioned by literature is turbulence, in the form of Froude and Reynolds numbers. First, I took the max depth and max velocity for four typical moments in the tidal cycle (Figure 20), to be sure the Froude numbers were calculated at the same location. The larger maximum depths had the largest flow velocities (Table 3), but it is interesting to see that de larger max flow velocity of Figure 20 d), which had only slightly higher water levels, coincided with a noticeably larger separation zone width. The Froude numbers, calculated with the formula:

$$Fr = \frac{u}{\sqrt{gh}} \quad (3)$$

are all below the values used by Bo and Ralston (2020), who considered Froude numbers between 0.1 and 0.2 to be small. To compare the values, I also calculated the Froude number at the boundary layer of the separation zone on 05/31, which gave a Froude number of $Fr = \frac{0.58}{\sqrt{g \cdot 9.01}} = 0.060$, slightly lower still than the values found in the channel. The Froude number is therefore not to be considered to be the major factor in determining whether or not flow separation occurs. The calculated Reynolds numbers are all in the same (high) order of magnitude for the four very different conditions, indicating that they too, are not an important factor in determining whether or not flow separation occurs in the Wester Scheldt estuary.

Table 3: Width of the separation zone, and the maximum water depths, maximum flow velocities, Reynolds and Froude numbers corresponding to the images shown in Figure 20. The width was taken along the dotted transect line, from the water edge to the boundary layer. The width of image c) was not determined, as the boundary layer was located at the edge of the submerged Ossenisse shoal, and the ebb return current had already started.

Image + date	Width	Max water depth	Max flow velocity	Reynolds number	Froude number
a) 05/31	226m	22.51m	1.06 m/s	$5.03 \cdot 10^9$	0.071
b) 06/04	47m	20.01m	1.03 m/s	$2.83 \cdot 10^9$	0.074
c) 06/13	-	24.15m	1.45 m/s	$9.10 \cdot 10^9$	0.094
d) 06/14	314m	22.61m	1.26 m/s	$6.46 \cdot 10^9$	0.085

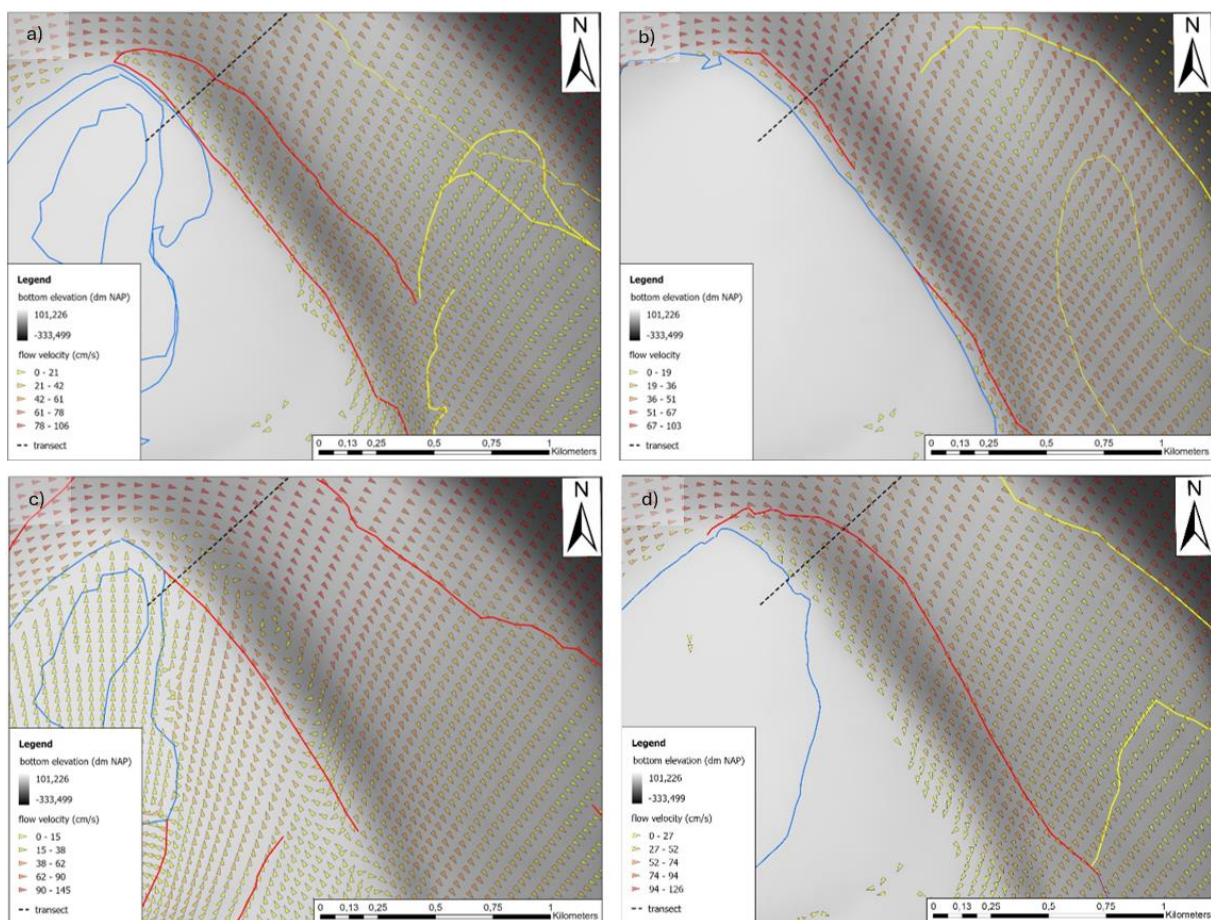


Figure 20: Ossenisse shoal with modelled flow velocities at four moments in the tidal flood phase. The dotted black line represents the transect over which the width of the separation zone is determined. a) 2023/05/31, 51cm NAP. b) LW at 2023/06/04, -199cm NAP. c) HW at 2023/06/13, 215cm NAP. Here the ebb-current has already started on the submerged Ossenisse shoal and it is at the shoal boundary, that the boundary layer was observed. d) 2023/06/14, 61cm NAP.

While Froude and Reynolds numbers were considered, I did not find any literature providing critical values of Reynolds numbers for flow separation. Blanckaert et al. (2013) found Reynolds numbers with orders of magnitude ranging from 10^5 to 10^6 , which is much lower than the values calculated for the Western Scheldt estuary. It is to be expected that flow velocity - which is included in the Reynolds number (equation 1) - plays a role in its development however, as flow velocity plays an important role in the momentum balance that steers the flow. Larger flow velocities result in a larger pressure gradient as more water is steered to the outer bend, and lead in turn to a greater pressure gradient lag behind inertial forces. Larger flow velocities

therefore logically would result in larger separation zones. This theory is supported by the finding that the width of the separation zone with larger flow velocities (Table 3), is larger than with lower velocities. This process is typically represented by the velocity component u (equation 1) in the Reynolds numbers, but the increase in Reynolds numbers found in the Western Scheldt estuary is limited and can not be expected to sufficiently portray this process.

4.4 Morphology

While R/w and Froude numbers appear to be poor predictors for flow separation, the location of flow separation is reasonably fixed in location. This suggests that the major contributor of flow separation is in fact the morphology, and thus the hydro-morphological feedback mechanisms in the estuary. The shallows around the shoals play a large role in the formation of flow separation, and mainly the shape of the shoals themselves. Figure 14 showed that with larger water depths, larger separation zones appeared. This was against the hypothesis that lower water levels in the inner bend would promote flow separation as the difference between flow velocities in the channel compared to near the shoal was larger. This hypothesis needs to be adjusted to the possible effect of inclination, rather than water depth, as a strong inclination might still prove to promote flow separation. Higher water levels appear to promote stronger flow separation zones however, which can be explained by the larger flow velocities that come with higher water levels. When at high water, the flow velocity drops, the separation zone east of the Ossenisse shoal logically disappears. The preexisting separation zone has at that point given rise to the start of the ebb tidal current. In rivers, it is to be expected that when flow velocities drop to a certain level, the separation zone might disappear completely, in estuaries, these zones are the first regions where the countercurrent will occur. A prime example of this is the apex of the Ossenisse shoal, which may be considered as a “sharp corner”, as separation zones appear in both ebb and flow directions. The shape of the Ossenisse shoal that incites flow separation, may in fact be formed by this same process of flow separation and according recirculation as schematised in Figure 21. While the flood flow erodes the west bank (21a), the decelerated or recirculating flow will deposit sediment at the east side. When the tide turns, this region is the first region where ebb flows start, which then erode the east side of the shoal, and causing deposition at the west side. The shallows east of the shoal and adjacent ebb-channel, may in fact be deposited by this mechanism. The triangular shape of the shoal is formed and maintained by a hydro-morphological feedback loop of erosion by the main flow, and deposition in the separation zone. Morphology is thus the main contributor to flow separation. These insights suggest that changing the morphology by depositing dredged material in the separating zone may reduce the flow separation, which may be useful for navigational safety and may be feasible in view of the large dredging volumes in the Western Scheldt. Before attempting this, research needs to be done to predict how the new morphology affects flow patterns elsewhere in the estuary. The complex flow patterns observed in Figures (16, 18) show how important it is

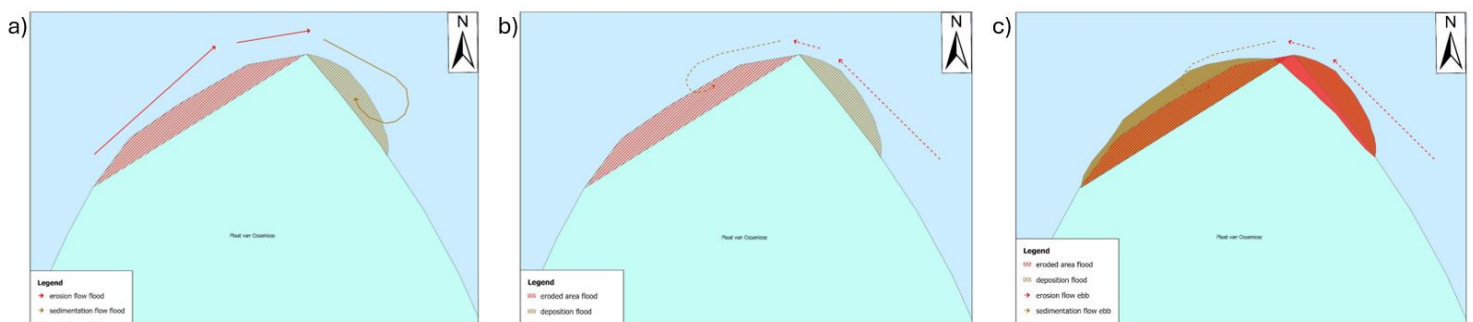


Figure 21: Schematic representation of morphology changes at the apex of the Ossenisse shoal. a) the flood current erodes the west side, and the recirculating or decelerating flow deposits sediment at the east side. b) the flow reverses. c) the ebb current erodes the east side and the recirculating or decelerating flow deposits sediment at the west side.

to have a thorough understanding of the hydro-morphological interactions when affecting either flow or morphology in the Western Scheldt, as one affects the other. Furthermore, when in future research the strength and width of the separation zone can be linked to the sedimentation rates and following flow rates, the size, strength and location of the zones may be better predicted and understood.

In this research, the main focus has been on the flood flow, because unfortunately, the quality of the images during the ebb flow, were not as good as those during flood. The effects on the development of the Ossensisse shoal could be theorized however. As water levels drop at the end of the ebb tidal phase, the region west of the shoal falls dry. When the tide turns, the flood flows will not be able to erode the western face of the shoal with a similar strength to the ebb flows. Following this logic, the separation zones in either direction around the apex of the Ossensisse shoal are strongest at high water levels, in other words in the beginning stages of the ebb flow, and at the end of the flood flow.

Conclusions

In the Western Scheldt estuary, hydro-morphological feedback mechanisms appear to be the dominant process in the development of flow separation. The persistence of the regions where flow separation occurs are evidence for the importance of morphology. Around the apex of the Ossenisse shoal, during flood, a separation zone is present, which grows wider and stronger with rising water levels. This contradicts with the hypothesis that the larger friction with lower water levels causes a larger difference between inner bend flow and outer bend flow. Inclination of the inner bend may still be of importance. Rising water levels lead to higher flow velocities which increase the pressure gradient that lags behind the inertial forces. Larger flow velocities therefore lead to more separation of flow. The separation zone east of the Ossenisse shoal has recirculation, which leads in turn to the start of the ebb-flow and an associated ebb-tidal channel. This early ebb-flow helps maintaining the shape of the Ossenisse shoal, which keeps its triangular shape and according *sharpness* thanks to the hydro-morphological feedback mechanisms. The bend ratio (normalized by channel width) of the bends, which played a crucial role in experimental research, has not been found to be of major value in predicting the existence of flow separation in the Western Scheldt, and the Froude and Reynolds numbers even less so. The effects of roughness could not be researched, but megaripples clearly respond to recirculating flow so feedback on the flow pattern remains of interest for future research.

Acknowledgements

I would like to thank Marco Schrijver for providing the model which showed flow velocities and bathymetry, Menno Straatsma and Maarten Zeijlmans for help with ArcGIS, and most importantly Maarten Kleinhans for his patience in supervising. Finally I would like to thank Anniek Stuuut and my parents for helping me through the post-covid struggle of writing a thesis, without them I would not have finished.

References

- Bagnold, R.A. 1960a. Geological Survey Professional Paper, 282 (E). Some aspects of the shape of river meanders. p. 135–144
- Bagnold, R.A. 1960b. Some aspects of the shape of river meanders. Geol. Surv. Prof. Pap. 282(E): 135–144. doi: 10.3133/pp282E.
- Blanckaert, K. 2010. Topographic steering, flow recirculation, velocity redistribution, and bed topography in sharp meander bends. *Water Resour. Res.* 46(9). doi: 10.1029/2009WR008303.
- Blanckaert, K. 2015. Flow separation at convex banks in open channels. *J. Fluid Mech.* 779: 432–467. doi: 10.1017/jfm.2015.397.
- Blanckaert, K. 2018. Hydro-sedimentological processes in meandering rivers: A review and some future research directions. *Fluv. Meand. Their Sediment. Prod. Rock Rec.:* 297–319. doi: 10.1002/9781119424437.CH12.
- Blanckaert, K., M.G. Kleinhans, S.J. McLelland, W.S.J. Uijttewaalt, B.J. Murphy, et al. 2013. Flow separation at the inner (convex) and outer (concave) banks of constant-width and widening open-channel bends. *Earth Surf. Process. Landforms* 38(7): 696–716. doi: 10.1002/esp.3324.
- Bo, T., and D. Ralston. 2020. Flow separation and increased drag coefficient in estuarine channels with curvature. *J. Geophys. Res. Ocean.* 125(10). doi: 10.1029/2020JC016267.
- Ferguson, R.I., D.R. Parsons, S.N. Lane, and R.J. Hardy. 2003. Flow in meander bends with recirculation at the inner bank. *Water Resour. Res.* 39(11). doi: 10.1029/2003WR001965.
- Hermans, M., K. Kauffman, S. Inda-Everts, T. de Jong, Y. Koldenhof, et al. 2022. Netwerkanalyse Noordzee 2022. Wageningen.
- James, C.S., W. Liu, and W.R.C. Myers. 2001. Conveyance of meandering channels with marginal vegetation. *Proc. Inst. Civ. Eng. Water Marit. Eng.* 148(2): 97–106. doi: 10.1680/WAME.2001.148.2.97.
- Kleinhans, M.G., B. Vermeulen, J.L. Best, J.H.. Candel, A.J.F. Hoitink, et al. 2023. Cutting Corners: Causes, Mechanisms and Large-Scale Effects of Sharp Bends in Rivers, Estuaries and Deltas. *JGR Earth Surf.:* 1–35.
- Leeder, M.R., and P.H. Bridges. 1975. Flow separation in meander bends. *Nature* 253(5490): 338–339. doi: 10.1038/253338A0.
- Marani, M., S. Lanzoni, D. Zandolin, G. Seminara, and A. Rinaldo. 2002. Tidal meanders. *Water Resour. Res.* 38(11): 7–1. doi: 10.1029/2001WR000404.
- Nanson, R.A. 2010. Flow fields in tightly curving meander bends of low width-depth ratio. *Earth Surf. Process. Landforms* 35(2): 119–135. doi: 10.1002/ESP.1878.
- Plancke, Y., J. Stark, D. Meire, and M. Schrijver. 2020. Complex Flow Patterns in the Scheldt Estuary: Field Measurements and Validation of a Hydrodynamic Model. *J. Hydraul. Eng.* 146(7): 1–15. doi: 10.1061/(asce)hy.1943-7900.0001737.
- Planet Team. 2023. Planet Application Program Interface: In Space for Life on Earth.
- Prandtl, L. 1952. *Essentials of fluid dynamics.* Blacky and Son Ltd.
- Rijkswaterstaat. Westerschelde - informatie en waterdata. <https://www.rijkswaterstaat.nl/water/vaarwegenoverzicht/westerschelde> (accessed 31 August 2024).
- Satellietdataportaal.nl Netherlands Space Office. 2023. Pléiades Neo.
- Simpson, R.L. 1989. Turbulent Boundary-Layer Separation. <http://dx.doi.org/10.1146/annurev.fl.21.010189.001225> 21(1): 205–232. doi: 10.1146/ANNUREV.FL.21.010189.001225.
- Vermeulen, B., A. Hoitink, and R. Labeur. 2015. Flow structure caused by a local cross-sectional area increase and curvature in a sharp river bend. *J. Geophys. Res. Earth Surface*, 2015 120(9): 1771–1783. doi: 10.1002/2014JF003334.

Wang, Z.B., C. Jeuken, and H.J. de Vriend. 1999. Tidal asymmetry and residual sediment transport in estuaries. A literature study and applications to the Western Scheldt. WL Delft Hydrolics (June 2014). <http://repository.tudelft.nl/assets/uuid:08911ef5-5ee8-4a8b-9432-5a5a5dfaa142/z2749dr.pdf>.